UDK 666.266.4:539.23
Original scientific article/Izvirni znanstveni članek

ISSN 1580-2949
MTAEC9, 57(6)607(2023)

PREPARATION AND PROPERTIES OF SiO_2/Ag MICROBEADS USING ELECTROLESS PLATING METHOD

PRIPRAVA IN LASTNOSTI SiO_2/Ag MIKRO KROGLIC Z METODO PLATIRANJA BREZ POMOČI ELEKTRIČNEGA TOKA

Congcong Zhang, Xiaolei Su*, Jiaqi Yan, Yi Liu

School of Materials Science & Engineering, Xi'an Polytechnic University, Xi'an 710048, China

Prejem rokopisa – received: 2023-01-31; sprejem za objavo – accepted for publication: 2023-09-18

doi:10.17222/mit.2023.778

SiO_2/Ag microbeads were synthesized using the electroless plating method by changing the addition order and the mixed method of electroless plating. Conducting composites were prepared using the prepared SiO_2/Ag microbeads and unsaturated polyester resin as the fillers and substrate, respectively. The microstructure and properties of the prepared microbeads and composite were characterized with a scanning electron microscope (SEM), X-ray diffractometer (XRD), energy dispersive spectrometer (EDS), particle size analyzer, DC milliohm meter and vector network analysis tester. Results show that the SiO_2/Ag microbeads prepared with the reverse dropping electroless plating method achieved the best uniformity and integrity of the silver coating on the surfaces of glass beads, and its compaction resistance reached 138.80 mΩ·cm. When the ratio of the prepared SiO_2/Ag microbeads and unsaturated polyester resin was 1:2, the obtained coating composite had a resistivity of 2.79×10^{-5} Ω·cm, showing good electromagnetic shielding performance.

Keywords: SiO_2/Ag microbeads, electroless plating, conductive coating, electromagnetic shielding

Steklene kroglice mikronske velikosti prevlečene s srebrom (angl.: SiO_2/Ag microbeads) so avtorji sintetizirali s fizikalno-kemijsko metodo oziroma platiranjem brez pomoči električnega toka (angl.: electroless plating). Pri tem so spremenili vrstni red postopkov in izbiro kemijske raztopine. Za izdelavo prevodnih kompozitov za prevleke so uporabili pripravljene SiO_2/Ag steklene mikro kroglice in nenasičeno poliestersko smolo kot polnilo oziroma podlago (substrat). Mikrostrukturo in lastnosti pripravljenih kroglic in kompozita so okarakterizirali s pomočjo vrstičnega elektronskega mikroskopaa (SEM), rentgenskega difraktometra (XRD), energijskega disperzijskega spektrometra (EDS), analizatorja velikostne porazdelitve delcev, merilnika električne upornosti (angl.: DC Milliohm Meter) in analizatorja za testiranje vektorske mreže. Rezultati analiz so pokazali, da imajo SiO_2/Ag kroglice mikronske velikosti, izdelane z večstopenjsko (povratno) mokro metodo platiranja (naprševanja) brez pomoči električnega toka odlično, homogeno in integrirano srebrno prevleko na površini steklenih kroglic. Kompaktna posteljica iz izdelanih SiO_2/Ag kroglic je imela upornost 138,8 mΩ·cm. Pri nasičenju oziroma razmerju 1:2 med izdelanimi SiO_2/Ag mikro kroglicami in nenasičenim poliestrom je imel izdelani kompozit za prevleke upornost $2{,}79 \times 10^{-5}$ Ω·cm. Tako izdelane kompozitne prevleke dobro ščitijo pred vplivom elektromagnetnega sevanja in so zato uporabne kot odlični oklopi (oklepi).

Ključne besede: posrebrene steklene kroglice, platiranje brez pomoči električnega toka, prevodne prevleke, elektromagnetno oklapljanje

1 INTRODUCTION

In recent years, potential safety hazards caused by electromagnetic radiation have attracted considerable attention due to the growth of the 5G technology and the application of telecommunication and electronic devices.[1–5] Among the plentiful kinds of materials for the electromagnetic shielding purpose, core-shell structured[6–8] conductive fillers consisting of SiO_2 cores and silver shells have been of momentous interest because of their light weight and good conductivity.[9] The conventional conductive fillers include silver-coated copper,[10] silver-coated aluminum[11], silver-coated nickel[12] powder, and so on. However, these composite powders are quite heavy,[13] and this limits their applications in lightweight designs. Glass microbeads have the advantages of exhibiting light weight, low thermal conductivity, high and low temperature resistance, corrosion resistance, good thermal stability,[14] high compressive strength, good dispersibility and fluidity; however, a bead itself has no conductivity or electromagnetic shielding characteristic.[15,16] As a result, scholars have made relevant research on silver plating of the surfaces of glass microbeads, discovering the excellent performance of core-shell structured fillers.[17–20]

So far, there have been many attempts to synthesize SiO_2/Ag composites,[21] involving the micro-emulsion method,[22] chemical reduction method,[23,24] sol-gel method,[25,26] thermal deposition,[27] electroless plating[28,29] and so on. In particular, the electroless plating method, which overcomes the problems of uneven mixing of the mechanical mixing method and easy grain growth of the sol-gel method in reducing alkali metal oxides, is widely used because it is not restricted to the material shape.[30,31] In addition it is a simple and easy-handling[4,30,31] process for the fabrication of silver-plated glass microbead composites with excellent performance. To this end, W.-J. Kim and S.-S. Kim[20] synthesized Ag-coated hollow

*Corresponding author's e-mail:
su_x_lei@163.com (Xiaolei Su)

microbeads using a two-step procedure of sensitizing and subsequent electroless plating. Wu et al.[32] prepared core-shell SiO_2/Ag composite microbeads with a dense, completive and scaled silver layer. However, SiO_2/Ag composites with a complete, uniform and compact silver shell and high-purity are still challenging to be gained.[32]

In this study, an optimal process for producing uniform, continuous, dense, complete silver[33] thin films with excellent electrical conductivity was investigated via altering the addition order and manner of electroless plating. Accordingly, the SiO_2/Ag core-shell particles[34] were fabricated with a smooth micro-morphology, low resistivity, strong stability, fine silver layer particles and high electromagnetic shielding energy. Meanwhile, probable reaction mechanisms for the formation of the SiO_2/Ag core-shell microbeads prepared with four electroplating addition methods were also discussed profoundly in this study. Subsequently, conductive coating composites were formed by combining SiO_2/Ag granules[35] and unsaturated polyester resin with screen printing technology. Finally, the EMI shielding performance and resistivity of the coating composites were tested, and the prepared conductive powder was tested via a scanning electron microscope, energy spectrometer, X-ray diffractometer, laser particle size analyzer, DC low resistance tester and other instruments.[36–38]

2 EXPERIMENTAL PART

2.1 Materials

Stannous chloride ($SnCl_2$) was purchased from Tianjin Kermel Chemical Reagent Co., Ltd., China. SiO_2 solid microbeads (≥99 %) with an average size of 48 μm were purchased from Hebei Jinghang Mineral Products Co., Ltd., China. Glucose ($C_6H_{12}O_6$) and tartaric acid ($C_4H_6O_6$) were obtained from Tianjin Tianli Chemical Reagents Co., Ltd., China. Silver nitrate ($AgNO_3$) and sodium hydroxide (NaOH) were procured from Damao Chemical Reagent Factory, China. Hydrofluoric acid (HF), absolute alcohol (C_2H_50H), sodium fluoride (NaF), hydrochloric acid (HCl) and ammonia water ($NH_3{\cdot}H_2O$) were supplied by Tianjin Hongyan Chemical Reagent Factory, China. Polyvinylpyrrolidone (PVP) was provided by Shanghai Aladdin Biochemical Technology Co., Ltd., China. The resin and deionized aqueous solutions were prepared in house. All the reagents and chemicals were of analytical grade and were used as received without further purification.

2.2 Preparation of SiO_2 microbeads

The SiO_2 microbeads (48 μm) were degreased with an NaOH solution, washed with deionized water three times and dried in a vacuum oven at 80 °C for 3 h for future use. In a while, the obtained microbeads were coarsened with a hydrofluoric acid and sodium fluoride mixture that was stirred at room temperature for 10 min at a stirring speed of about 350 min^{-1}, rinsed with deionized water and dried for future use. The aim of the coarsening reaction was to corrode the surfaces of SiO_2 microbeads, thus increasing the surface roughness and specific area.

The coarsened microbeads (40 g) were sensitized in a stannous chloride and hydrochloric acid mixture solution containing 6.4 g $SnCl_2$ + 24 mL HCl + 320 mL distilled water. Afterward the microbeads were sluiced with distilled water, vacuum filtered and dried in the vacuum oven at 80 °C for 3 h.[39] The sensitizing reaction allowed the attachment of a layer of a Sn^{2+} film to the SiO_2 surfaces, providing reducing substances for the next step.[39]

The sensitized microbeads (10 g) were activated in a silver ammonia solution ($Ag(NH_3)_2OH$ 2.5 g/L) that was shaken uniformly at 40 °C for 25 min at a stirring speed of about 350 min^{-1}. Then, the microbeads were washed with distilled water, vacuum filtered and dried at 80 °C. A tier of Sn^{2+} ions[40] adsorbed on the surfaces of silica microbeads reacts with the silver ammonia solution, and $[Ag(NH_3)_2]^+$ ions[32] are reduced to Ag particles that are uniformly adhered onto the surfaces of microbeads. The newly reduced Ag particles on the silica surface act as the seeds which provide nucleation sites for a new deposition and growth of the silver shell.[20,32]

A schematic diagram of the pretreatment process of SiO_2 microbeads is shown in **Figure 1**. SiO_2 is a microbead with a smooth surface. After a variation in the mixed solution with hydrofluoric acid and sodium fluoride, the surface of SiO_2 becomes rough and the specific surface area increases. The rough surface is of great benefit to the adhesion of the Sn^{2+} film[39] and SiO_2 substrate

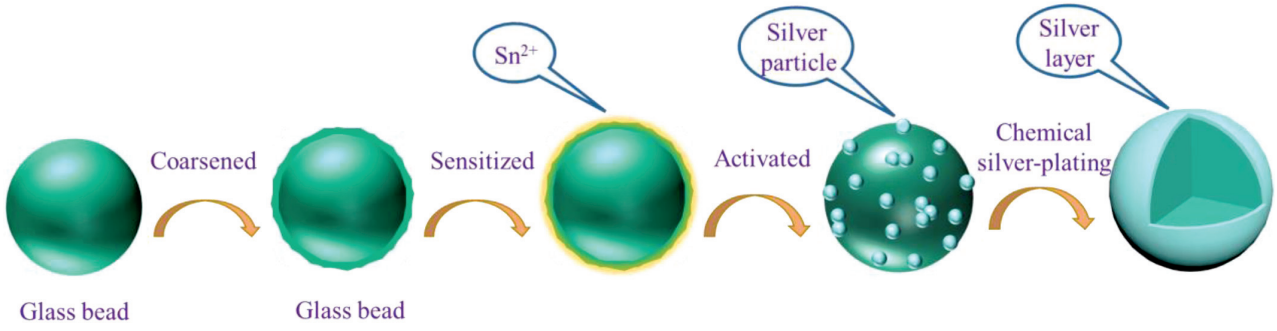

Figure 1: Schematic diagram of the pretreatment process

during the sensitization process. Besides, a large specific surface area provides sites for the Ag seed deposition.[41] The Sn^{2+} film can supply reducing substances which react with the silver ammonia solution used in the activation process to generate silver particles as active sites[41]. After the deposition of Ag seeds on the glass microbeads, the silver particles are gradually and continuously attached to the surface of SiO_2 to form a SiO_2/Ag core-shell structure composite via the chemical silver-plating method.

2.3 Synthesis of SiO_2/Ag microbeads

The SiO_2/Ag core-shell particles were synthesized through the electroless plating method. In brief, the sensitized microbeads were put in a plating solution containing an oxidizing agent (silver nitrate – $AgNO_3$), a reducing agent (glucose – $C_6H_{12}O_6$), a stabilizing agent (ethanol – C_2H_50H), a dispersing agent (polyvinylpyrrolidone – PVP), a PH control agent (sodium hydroxide – NaOH) and distilled water. The reducing agent was a mixture of glucose and tartaric acid. The mixing ratio of glucose to tartaric acid was 1:8 by weight. The plating solution was agitated at 40 °C for 20 min, then the NaOH solution was dropwise added into the reaction solution and stirred for 20 minutes in order to adjust the pH value of the solution. After reacting, the Ag-coated microbeads were gravity filtered,[41] rinsed with distilled water and dried at 80 °C in the vacuum oven. After thorough filtering, rinsing and drying, the SiO_2/Ag core-shell granules were successfully obtained.

In the experiment, four ways of forward dropping, forward mixing, reverse dropping and reverse mixing were used for the electroless silver plating of the pretreated microbeads. A schematic diagram of the adding method of electroless plating is shown in **Figure 2**. The best preparation parameters obtained through experiments are as follows: $AgNO_3$ – 15 g/L, an appropriate amount of ammonia water, $C_6H_{12}O_6$ – 10 g/L, C_2H_5OH – 40 mL/L, PVP – 2 g/L, reaction temperature – 40 °C, PH = 11.

2.4 Fabrication of the SiO_2/Ag coating composite

The SiO_2/Ag coating composites were prepared using the screen printing technology, and the ratio of SiO_2/Ag microbeads to unsaturated polyester resin was 1:2 by weight. Firstly, a ceramic rectangular piece was fixed firmly on a screen printer. Then a mixed sizing agent was applied on the ceramic sheet with a scraper. Finally, the ceramic piece was taken out and put into a Petri dish, then dried at 120 °C for 2 h in the vacuum oven. All samples of the SiO_2/Ag coating composite manufactured with the screen printing technology were cut into a rectangular block with a size of 2.0 cm × 2.0 mm × 0.12 mm.[42]

2.5 Characterization

The morphologies of SiO_2/Ag microbeads were investigated using a field emission scanning electron microscope (FE-SEM, Quanta-450-FEG+X-MAX50, FEI Company, Netherlands), operating at an accelerating voltage of 30 kV. The compositional information of the silver-plated glass microbeads was acquired with an energy dispersive spectrometer (EDX, Horiba 7021-H2, SUPU, China) installed on FE-SEM. The crystalline structure and the phase composition of the prepared composites were characterized via X-ray diffraction (XRD, DX-2700BH, Dandong Haoyuan Instrument Co., Ltd., China) under a CuK_α radiation (λ = 1.5400 nm) at a scanning range (2θ) of 10–90° and a step size of 0.03°.

The particle size and its distribution in the powder were measured with a laser particle size analyzer (JB6100-A, Shanghai Jiubin Instrument Co., Ltd., China) in a size number range of 0.01–1250 μm. The compaction resistance of SiO_2/Ag core-shell microbeads was tested with a DC milliohm meter (TH2516, Tonghui, China). The resistivity of the conductive coating was gauged as follow:

$$\rho = RS/L \tag{1}$$

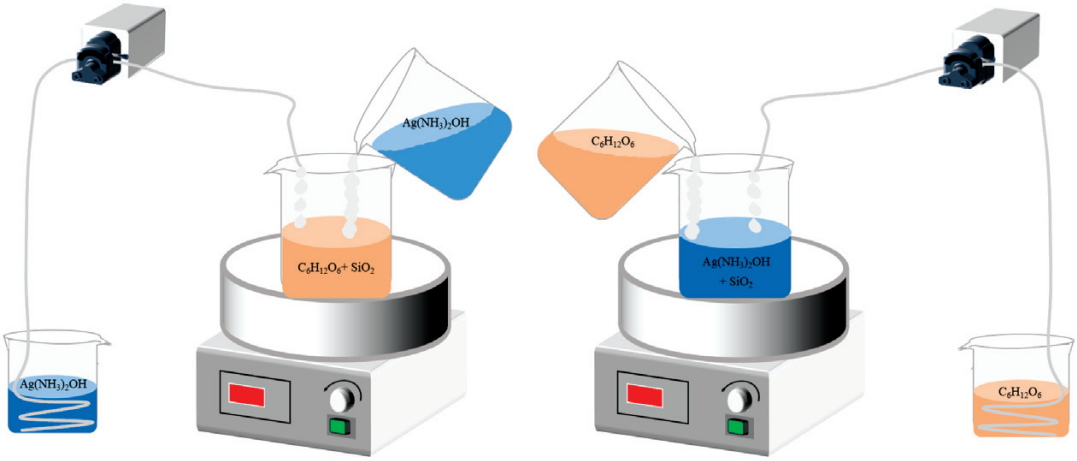

Figure 2: Schematic diagram of the adding method of electroless plating

where R is the resistance, S is the cross-sectional area and L is the length.

The electromagnetic interference (EMI) shielding properties of the conductive coating composite were tested with a vector network analyzer (Keysight E5061B ENA, Shenzhen, China), using the waveguide method within 0.5–6 GHz. The S parameter of electromagnetic shielding was obtained with the vector network analyzer, while the transmittance (T), reflectance (R) and absorptivity (A) were analyzed based on the S parameter.[43–45] S_{11} represents the reflection coefficient on plane T_1; S_{21} represents the forward transmission coefficient from plane T_1 to plane T_2.

$$R = |S_{11}|^2 \, , \; T = |S_{21}|^2 \tag{2}$$

$$A = 1 - R - T \tag{3}$$

The overall electromagnetic interference shielding effectiveness (SE) of the coating composite was calculated as follows:

$$SE = SE_R + SE_A + SE_M \tag{4}$$

$$SE_R = -10 \log (1 - R) \tag{5}$$

$$SE_A = -10 \log (T / (1 - R)) \tag{6}$$

where SE_R is the microwave reflection, SE_A is the microwave absorption and SE_M is the microwave multiple reflection. When SE = 15 dB, the SE_M can be insignificant.[13,43–45]

3 RESULTS AND DISCUSSION

3.1 Micromorphology and characterizations of SiO_2/Ag microbeads

3.1.1 Surface micromorphology

The surface micro-morphology of the core-shell SiO_2/Ag microbeads obtained with different electroless plating methods and under the same magnification of SEM observation is shown in **Figure 3**. As indicated in **Figure 3a**, the coating prepared with forward dropping is relatively uniform and complete, while the appearance of SiO_2/Ag is a little rough because of uneven growth of silver particles. It is found that there is a lot of agglomeration[33] of white flocs around the silver-plated glass microbeads in **Figure 3b** where the silver applied with forward mixing on the glass microbead surfaces is not uniform. When comparing **Figures 3c** and **3b**, it is obvious that no white flocs are produced near the surfaces of SiO_2/Ag microbeads on the former figure where the silver coating is complete and compact. It is also worth noting that **Figure 3c** shows a SEM image of silver-plated silica microbeads with a smooth surface and homogeneous size. In **Figure 3d**, the silica microbeads are also completely covered by consecutive silver particles, while the coating effect of the SiO_2/Ag core-shell particles synthesized via reverse mixing is relatively poor.

The mechanism diagram of the silver layer growth process is shown in **Figure 4**. There are two explanations for the reduction mechanism of Ag^+. Some scholars think that silver is deposited via a non-autocatalytic process and can be deposited by itself in a solution. Others believe that silver still has an autocatalytic effect, but the catalytic ability is not strong enough so it is necessary to activate SiO_2 microbeads before silver particles are continuously attached on the substrate surface.

The specific synthetic mechanisms of the two forward electroless silver plating methods are as follows. Pure silver particles can be relatively uniformly attached and deposited on the surfaces of glass microbeads because the reaction rate via dropping in the forward direction is slow. Furthermore, the oxidation-reduction reaction is generally carried out on the surfaces of microbeads. Meanwhile, the substrate is a glucose solution under this circumstance, which does not form new silver pure elements with the silver nitrate solution as the active site of electroless silver plating so that the preferential growth of Ag occurs in some parts of SiO_2 surfaces and the silver shell coating is not uniform. In contrast, the oxidation-reduction reaction rate with forward mixing is too fast, leading to quantities of silver elementary substances in the solution in the form of aggregation. To be specific, before most silver ions reach the surfaces of glass beads, they first react in the electroless plating solution and then form silver elementary substance aggregations in the solution. Only a small amount of silver ions[34] react on the surfaces of glass beads, which results in a large number of white flocculent silver elements around SiO_2/Ag while most of the glass beads are not completely covered with Ag layers.

Moreover, the explicit synthetic mechanisms of the two reverse chemical silver-plating methods are also clarified. A comparatively mild reaction rate during reverse dropping promotes a uniform deposition of Ag particles and makes Ag cover the silica surface completely to form a silver shell.[46] In this case, the silver ammonia solution as the matrix can cause a redox reaction on the surfaces of activated microbeads, forming a thin layer of silver coating that provides stable active sites for an argentic growth in the subsequent Ag plating process.

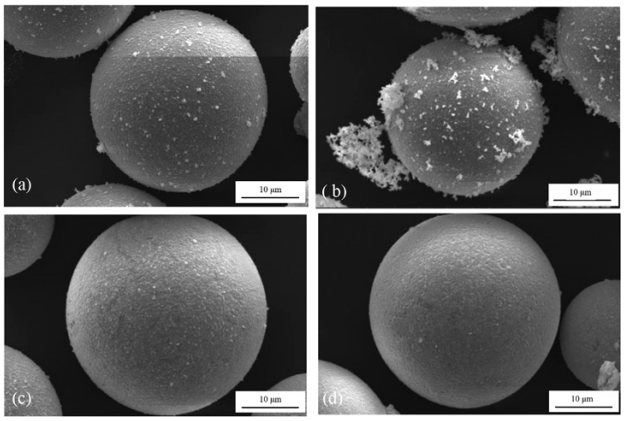

Figure 3: SEM images of SiO_2/Ag microsbeads: a) forward dropping, b) forward mixing, c) reverse dropping, d) reverse mixing

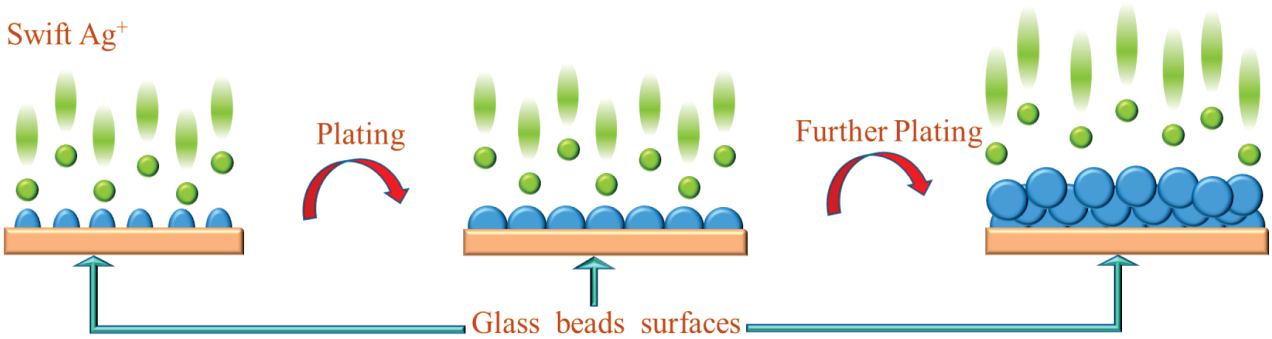

Figure 4: Mechanism diagram of the silver layer growth process

With an increased plating time, Ag particles are deposited more uniformly onto the SiO_2 surface, gradually forming a core-shell structure, and eventually the covered silver-coated silica beads become complete, uniform and compact. When the reverse mixing method is adopted, the preferential growth of silver ions during the crystallization procedure may lead to aggregated lumps and uneven silver layers on the surface.[32] It is also possible that the mixing reaction starts at a very fast rate so that the growth of silver immediately reaches saturation, which makes the silver nucleate rapidly. During the continuation of chemical silver plating, the concentration of the reaction solution decreases and the silver enters the growth stage, resulting in the separation of nucleation and growth of silver, and thus silver lumps appear somewhere on the surface as shown in **Figure 3d**.

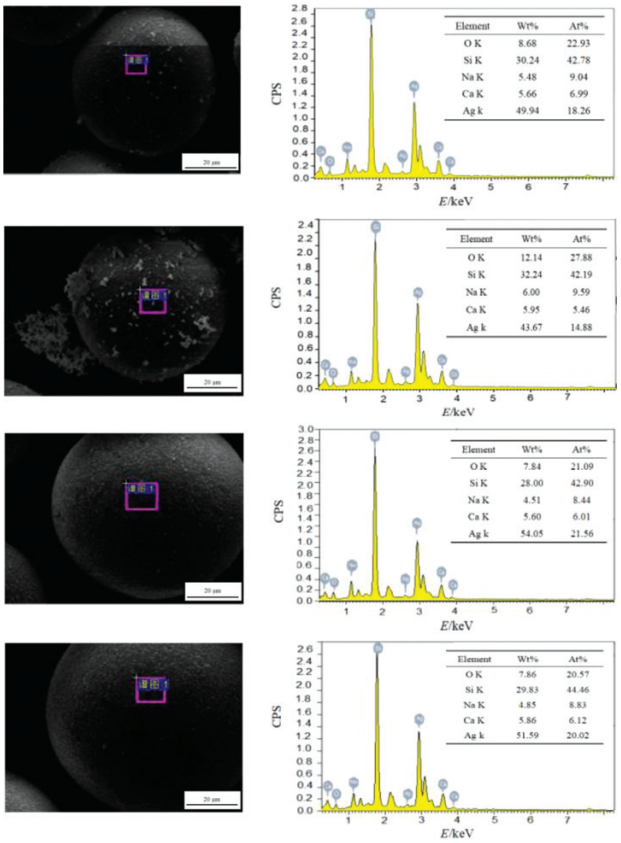

Figure 5: SEM images with marked EDS measurement areas and EDS spectra of SiO_2/Ag microbeads: a) forward dropping, b) forward mixing, c) reverse dropping, d) reverse mixing

3.1.2 EDS characterization

The chemical compositions of SiO_2/Ag microbeads prepared with the reaction methods with different addition orders were analyzed using an energy dispersive X-ray spectrometer (EDS) as shown in **Figure 5**. As can be seen on this figure, only Si, O, Ca, Na and Ag peaks are clearly shown and no other peaks are detected. The content of Ag on the surface of SiO_2/Ag is about (49.9, 43.7, 54.1 and 51.6) *w*/% when the preparing methods are forward dropping, forward mixing, reverse dropping and reverse mixing, respectively. This means that an Ag shell with a high purity was acquired on silica microbeads in the current study.

3.1.3 XRD characterization

The spectra in **Figure 6** show typical X-ray diffraction (XRD) patterns of silver-plated glass beads prepared with the four reaction methods with different addition orders to verify the crystalline properties and phase purity of the obtained samples. The four well-resolved diffraction peaks of SiO_2/Ag core-shell composites are observed at 2θ angles of 38.12°, 44.30°, 64.44° and 77.40°, in a range of approximately 30–80°, corresponding to the reflections of the (111), (200), (220) and (311) crystal

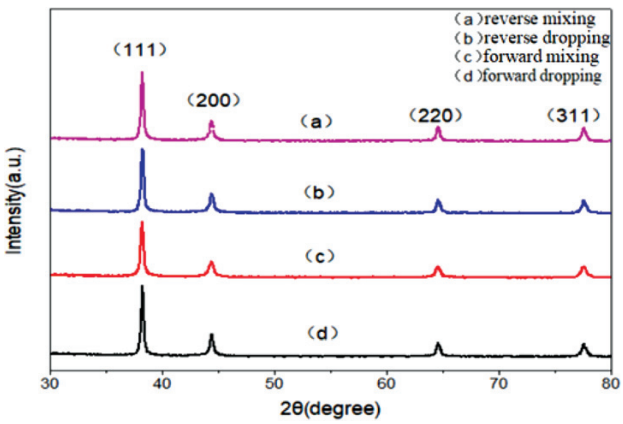

Figure 6: X-ray diffraction patterns of SiO_2/Ag microbeads

planes of face-centered cubic (FCC) metal silver (JCPDS Card No. 87-0720), respectively.[31,32,47] There is no diffraction peak of silver compounds, indicating that the pure Ag particles with high crystallinity were deposited to grow on the Ag seeds on the surface of SiO_2.[48] These XRD results agree well with those of SEM observations.

3.2 Particle size of SiO_2/Ag microbeads

The particle sizes of SiO_2/Ag microbeads prepared with different electroless plating methods are shown in **Figure 7**. It can be seen that the particle magnitude range obtained for the experimental glass microbeads is about 20–67 μm and its D50 is about 34 μm[49]. It is also clear from the figure that there is almost no big difference between the average particle sizes of the samples prepared with the four methods. In addition, the total number of particles below 5 μm in silver plated glass microbeads produced with the reverse method is larger than that obtained with the forward method. This is because there are a few dissociative silver particles in the forward reaction process, leading to an increase in the accumulation of ultra-fine particles,[50,51] while the cumulant of the silver-plated glass microbeads in this size range is relatively limited in the reverse course of reaction. It can be further explained that silver grows better on the surfaces of glass microbeads during reverse electroless silver plating.

3.3 Measurement of resistance of SiO_2/Ag microbeads

The compaction resistance of SiO_2/Ag conductive microbeads is shown in Table 1. It can be clearly seen that the electric resistance of the sample obtained with forward mixing is the highest, while that of the sample obtained with reverse mixing is the lowest.[46]

3.4 Measurement of resistivity of SiO_2/Ag coating composites

The conductive coatings composed of SiO_2/Ag microbeads were made using the screen printing technology, and its parameters were 2.0 cm, 2.0 mm, 0.12 mm in length, width and thickness, respectively. The mass ratio of SiO_2/Ag microbeads to unsaturated polyester resin was 1:2. The resistance of these coatings was tested with a DC milliohm meter and then the resistivity of the layers was calculated. The testing information is shown in **Table 2**. It is clearly seen that the resistivity of the SiO_2/Ag coating composite obtained with forward mixing is the largest, and the one prepared by reverse dropping is relatively small, with values of 3.64×10^{-5} Ω·cm and 2.79×10^{-5} Ω·cm, respectively. It is also worth noting that the resistivity of the SiO_2/Ag coating obtained with reverse mixing is smaller than that obtained with reverse dropping, which is consistent with the result for the compaction resistance of SiO_2/Ag microbeads.

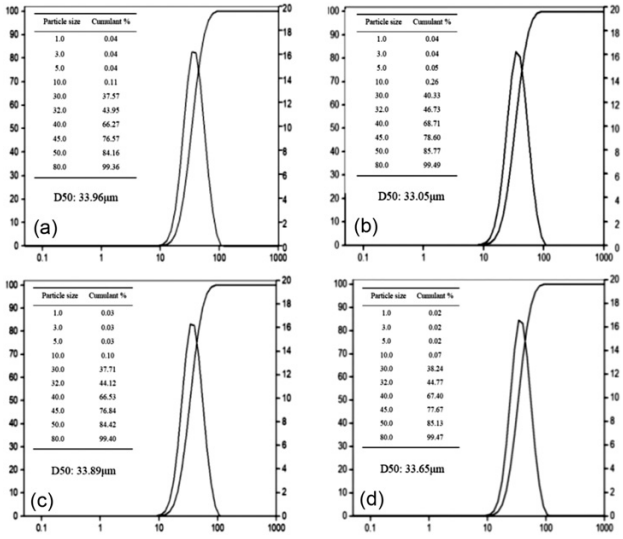

Figure 7: Particle size of SiO_2/Ag microbeads: a) fForward dropping, b) forward mixing, c) reverse dropping, d) reverse mixing

Table 1: Compaction resistance of SiO_2/Ag microbeads

Reaction method	Forward dropping	Forward mixing	Reverse dropping	Reverse mixing
Sample color	Gray white	Grey	Off white	Gray white
R/mΩ·cm	138.50	142.10	138.80	137.75

Table 2: Average resistance and resistivity of SiO_2/Ag coating composites

Reaction method	Average resistance /Ω	Resistivity /Ω·cm
Forward dropping	2.685	3.22×10^{-5}
Forward mixing	3.036	3.64×10^{-5}
Reverse dropping	2.324	2.79×10^{-5}
Reverse mixing	2.129	2.55×10^{-5}

The resistance of the samples obtained with forward mixing is the highest, while that of the microbeads and its coating obtained with reverse mixing is the lowest. This may be because the matrix is a silver ammonia solution which first reacts with the substance on the surfaces of the glass microbeads, and then the thin layer of Ag is reduced to supply active sites[20] for the subsequent electroless plating during the reverse reaction process. However, the active sites are relatively insufficient in the forward reaction process, leading to a comparatively unsatisfactory coating effort, resulting in an enhancement of the resistance values.

The reason why the resistance of the microbeads prepared with reverse mixing addition is better than that obtained with reverse dropping addition may be as follows. At the beginning of the reaction, the speed of reverse mixing was fast, and in the meantime the silver generation rate had reached saturation, resulting in a rapid nucleation. Afterwards, with a decrease in the reaction concentration, the reaction rate began to slow down, and the nucleation and growth were basically separated, resulting in the phenomenon of explosive nucleation and slow

growth.[52] In addition, too slow a rate at the later stage of reverse mixing reaction may have also brought about the preferential growth of silver, leading to an aggregation of Ag particles on the surfaces of microbeads. Because of the existence of silver nuggets, the resistance of the SiO_2/Ag microbeads and coating composites gained with reverse mixing is smaller than that obtained with reverse dropping.

3.5 Electromagnetic shielding performance of SiO_2/Ag conductive coatings

In this experiment, a shielding test was conducted in an electromagnetic wave frequency range of 0.5–6 GHz. The electromagnetic shielding effectiveness of the SiO_2/Ag conductive coating is shown in **Figure 8**. The common trend of the four curves indicates that the SE_R value increases as the frequency of electromagnetic waves decreases, significantly increasing from (45.10, 45.6, 46.25 and 46.63) dB to (55.88, 56.42, 57.05 and 57.43) dB due to the electroless Ag-plating methods including forward mixing, forward dropping, reverse dropping and reverse mixing, respectively. When the waves are shorter than 1 GHz, the electromagnetic shielding of SiO_2/Ag coatings exhibits a comparatively high performance with a SE_R value exceeding 52 dB. Detailed relationship between the electromagnetic shielding effectiveness and efficiency can be found in **Table 3**.[53] According to the experimental results and measurements, the shielding efficiency of all four kinds of SiO_2/Ag conductive coatings is 99.999 %.

It is obvious from **Figure 8** that the electromagnetic shielding effectiveness of the conductive coating prepared with the reverse mixing method is the best, while the one obtained with the forward mixing method is the poorest. Moreover, the shielding curves of the conductive coatings prepared with reverse dripping and reverse mixing are very close. It is well known that the electromagnetic shielding performance increases with a decrease in the resistance and resistivity. This result agrees well with those of resistance and resistivity measurements, and the phenomenon, according to which the shielding curve of the SiO_2/Ag coating obtained with reverse mixing is slightly higher than that obtained for reverse dropping, is caused by the presence of silver nuggets on the SiO_2/Ag powder surface. The complex conductive coating is composed of many SiO_2/Ag microbeads, which connect with each other to form a continuous conductive network. The increase in the SE_R of these four different SiO_2/Ag coatings is ascribed to the content, uniformity and integrity of the silver adhered over the SiO_2 microbeads.

As incident electromagnetic waves run into the coarse Ag layers, they are diminished by scattering, adsorption and reflection many times in the formed conductive network. The electromagnetic field can induce currents resulting in ohmic losses, effectively shielding the electromagnetic waves.[43] From the above analysis, we can conclude that the electromagnetic shielding effectiveness of the conductive layer changes with the adjustment of the adding modes when the values for the electromagnetic shielding effectiveness of the coatings consisting of SiO_2 microbeads produced through reverse mixing and dropping are slightly different and the shielding efficiency is good.

Table 3: Relationship between electromagnetic shielding effectiveness and efficiency[53]

Effectiveness (dB)	Efficiency (%)
0	0
10	90
20	99
30	99.9
40	99.99
50	99.999
60	99.9999
70	99.99999
80	99.999999
90	99.9999999
92	99.99999994

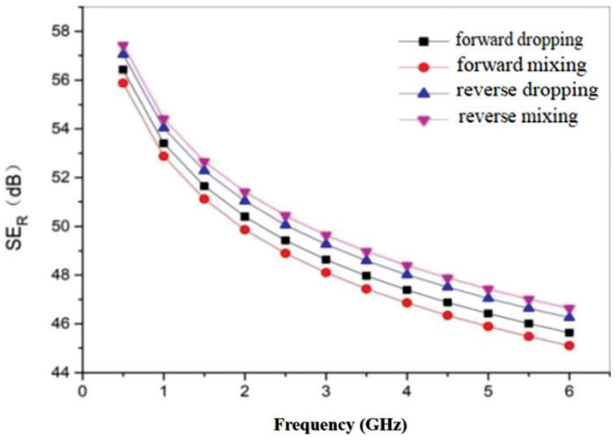

Figure 8: Electromagnetic shielding effectiveness of SiO_2/Ag coating composite

4 CONCLUSIONS

High-performance SiO_2/Ag core-shell composites with both superior surface topography and electromagnetic shielding properties were successively synthesized via the reverse dropping electroless plating method and utilized as conductive fillers to manufacture a SiO_2/Ag conductive coating.[41] Their microstructure, chemical composition, phase composition, particle size, conductivity and electromagnetic interference shielding properties were investigated. The results of SEM, EDS, XRD, particle size analyzer and DC milliohm meter showed that SiO_2 microbeads were covered with a uniform, continuous, complete and compact Ag shell, which allowed silver-plated glass beads to have good conductivity; its compaction resistance was 138.80 mΩ·cm, the silver layer had an fcc structure, and its D50 was about 34 μm.

The results also showed that the effect of reverse electroless Ag-plating was better than that of a forward reaction, and the coating effect of dropping was better than that of mixing. Almost no white flocs were produced on the surfaces of silver-plated glass beads prepared with the reverse dropping method, and the coating was dense, uniform and complete.[6] Besides, the Ag content of the coating was relatively high, reaching about 54.1 *w*/%, and the silver shells did not fall off easily.

By analyzing the silver layer growth and SiO_2/Ag microbead synthesis mechanisms, it can be concluded that both the reaction speed and reactant addition order had a major impact on the deposition and growth of silver particles where neither too fast nor too slow a reaction rate was conducive to electroless Ag-plating. In this system of taking Ag-seeds as active sites of Ag-shell growth, surface morphologies and application performances of the micro-composites can be well controlled and regulated by changing the addition order and using the mixed method of electroless plating. The prepared coating composite fabricated of unsaturated polyester resin and SiO_2/Ag, obtained through reverse dropping, with a ratio of 1:2, exhibits excellent electromagnetic shielding performance[54–56] including a resistivity of 2.79×10^{-5} Ω·cm, SE_R value of 57.05 dB and wave frequency range of 0.5–6 GHz. This result is mainly attributed to the formation of a conductive path and improvement of electrical conductivity through SiO_2/Ag core-shell[18] particles acting as the conductive fillers. In conclusion, the SiO_2/Ag microbeads obtained with reverse dropping have great potentials and promising applications in the field of EMI shielding.

Acknowledgments

The authors gratefully acknowledge support from the Scientific Research Program Funded by Education Department of Shaanxi Provincial Government (Program No.23JC036) and Scientific and Technological Plan Project of Xi'an Science and Technology Bureau (Program No. 23KGDW0031-2022).

5 REFERENCES

[1] S. Wei, C. Zhou, L. Huang, Occupational health and safety: measurement and analysis of the electromagnetic radiation produced by radiofrequency devices for rejuvenation, Lasers Med Sci, 38 (**2022**) 1, 25–25, doi:10.1007/s10103-022-03669-y

[2] T. Zhang, D. Wang, R. Liu, Y. Xie, J. Li, L. Wang, A Coral Reef-Like Structure Fabricated on Cellulose Paper for Simultaneous Oil-Water Separation and Electromagnetic Shielding Protection, ACS Omega, 5 (**2020**) 29, 18105–18113, doi:10.1021/acsomega.0c01666

[3] K. Karipidis, R. Mate, D. Urban, R. Tinker, A. Wood, 5G mobile networks and health – a state-of-the-science review of the research into low-level RF fields above 6 GHz, J. Expo. Sci. Environ. Epidemiol., 31 (**2021**) 4, 585–605, doi:10.1038/s41370-021-00297-6

[4] R. P. Chowdhury, L. A. Stegeman, M. L. Lund, D. Fry, S. Madzunkov, A. A. Bahadori, Hybrid methods of radiation shielding against deep-space radiation, Life Sciences in Space Research, 38 (**2023**), 67–78, doi:10.1016/j.lssr.2023.04.004

[5] Z. Ding, X. Xiang, J. Li, S. Wu, Molecular Mechanism of Malignant Transformation of Balb/c-3T3 Cells Induced by Long-Term Exposure to 1800 MHz Radiofrequency Electromagnetic Radiation (RF-EMR), Bioengineering (Basel), 9 (**2022**) 2, 43–43, doi:10.3390/bioengineering9020043

[6] Q. Wu, H. Zhang, Y. Zhou, Z. Tang, B. Li, T. Fu, Y. Zhang, H. Zhu, Core-Shell Structured Carbon@Al_2O_3 Membrane with Enhanced Acid Resistance for Acid Solution Treatment, Membranes (Basel), 12 (**2022**) 12, 1246–1246, doi:10.3390/membranes12121246

[7] Y. Bao, X. Wu, B. Yin, X. Kang, Z. Lin, H. Deng, H. Yu, S. Jin, S. Chen, M. Zhu, Structured copper-hydride nanoclusters provide insight into the surface-vacancy-defect to non-defect structural evolution, Chem. Sci., 13 (**2022**) 48, 14357–14365, doi:10.1039/d2sc03239b

[8] C. Wang, D. Ma, X. Li, D. Luo, L. Wu, An electroless-plating-like solution approach for the preparation of PS@TiO2@Ag core-shell spheres, RSC Adv., 10 (**2020**) 16, 9341–9346, doi:10.1039/c9ra10624c

[9] B. Guo, J. Liang, J. Chen, Y. Zhao, Highly flexible and ultrathin electromagnetic-interference-shielding film with a sandwich structure based on PTFE@Cu and Ni@PVDF nanocomposite materials, RSC Adv., 12 (**2022**) 46, 29688–29696, doi:10.1039/d2ra05439f

[10] S. Lee, C. Wern, S. Yi, Novel Fabrication of Silver-Coated Copper Nanowires with Organic Compound Solution, Materials (Basel), 15 (**2022**) 3, 1135–1135, doi:10.3390/ma15031135

[11] M. Hao, L. Li, X. Shao, M. Tian, H. Zou, L. Zhang, W. Wang, Fabrication of Highly Conductive Silver-Coated Aluminum Microspheres Based on Poly(catechol/polyamine) Surface Modification, Polymers (Basel), 14 (**2022**) 13, 2727–2727, doi:10.3390/polym14132727

[12] Y. Yang, G. Montserrat-Siso, B. Wickman, P. A. Nikolaychuk, I. L. Soroka, Core-shell and heterostructured silver-nickel nanocatalysts fabricated by gamma-radiation induced synthesis for oxygen reduction in alkaline media, Dalton Trans., 51 (**2022**) 9, 3604–3615, doi:10.1039/d1dt03897d

[13] X.-K. Lv, J.-G. Yu, Novel Silver-Plated Nickel-Coated Graphite Powder with Excellent Heat and Humidity Resistance: Facile Preparation and Performance Investigation, Molecules, 27 (**2022**) 13, 4007–4007, doi:10.3390/molecules27134007

[14] C. P. Feng, F. Wei, K. Y. Sun, Y. Wang, H. B. Lan, H. J. Shang, F. Z. Ding, L. Bai, J. Yang, W. Yang, Emerging Flexible Thermally Conductive Films: Mechanism, Fabrication, Application, Nano-Micro Letters, 14 (**2022**) 1, 127–127, doi:10.1007/s40820-022-00868-8

[15] Y. Ma, H. Liu, Z. Han, L. Yang, J. Liu, Highly-reproducible Raman scattering of NaYF4:Yb,Er@SiO2@Ag for methylamphetamine detection under near-infrared laser excitation, Analyst, 140 (**2015**) 15, 5268–5275, doi:10.1039/c5an00441a

[16] X. G. Cao, H. Y. Zhang, Investigation into conductivity of silver-coated cenosphere composites prepared by a modified electroless process, Applied Surface Science, 264 (**2013**), 756–760, doi:10.1016/j.apsusc.2012.10.116

[17] H. Wang, F. Fotovat, X. T. Bi, J. R. Grace, Tribo-charging of binary mixtures composed of coarse and fine particles in gas-solid pipe flow, Particuology, 43 (**2019**), 101–109, doi:10.1016/j.partic.2018.07.001

[18] K. Siczek, H. Zatorski, A. Chmielowiec-Korzeniowska, R. Kordek, L. Tymczyna, J. Fichna, Evaluation of anti-inflammatory effect of silver-coated glass beads in mice with experimentally induced colitis as a new type of treatment in inflammatory bowel disease, Pharmacological Reports, 69 (**2017**) 3, 386–392, doi:10.1016/j.pharep.2017.01.003

[19] K. Siczek, J. Fichna, H. Zatorski, B. Karolewicz, L. Klimek, A. Owczarek, Development of the rectal dosage form with silver-coated glass beads for local-action applications in lower sections of the gastrointestinal tract, Pharmaceutical Development and Technology, 23 (**2018**) 3, 295–300, doi:10.1080/10837450.2017.1359843

[20] W.-J. Kim, S.-S. Kim, Preparation of Ag-coated hollow microspheres via electroless plating for application in lightweight microwave absorbers, Applied Surface Science, 329 (**2015**), 219–222, doi:10.1016/j.apsusc.2014.12.173

[21] C. Liu, D. Yang, Y. Jiao, Y. Tian, Y. Wang, Z. Jiang, Biomimetic synthesis of TiO_2-SiO_2-Ag nanocomposites with enhanced visible-light photocatalytic activity, ACS Appl. Mater. Interfaces, 5 (**2013**) 9, 3824–3832, doi:10.1021/am4004733

[22] F. Jiang, X. X. Wei, J. Zheng, Synthesis and electromagnetic characteristics of MnFeO/TiO composite material, Materials Research Express, 9 (**2022**) 10, doi:10.1088/2053-1591/ac97de

[23] G. Yang, S. Luo, T. Lai, H. Lai, B. Luo, Z. Li, Y. Zhang, C. Cui, A Green and Facile Microvia Filling Method via Printing and Sintering of Cu-Ag Core-Shell Nano-Microparticles, Nanomaterials, 12 (**2022**) 7, 1063, doi:10.3390/nano12071063

[24] Z. Wang, K. Yliniemi, B. P. Wilson, M. Lundstom, Targeted surface modification of Cu/Zn/Ag coatings and Ag/Cu particles based on sacrificial element selection by electrodeposition and redox replacement, Surface & Coatings Technology, 441 (**2022**), doi:10.1016/j.surfcoat.2022.128531

[25] P. Karo-Karo, S. Sembiring, I. Firdaus, R. Situmeang, S. D. Yuwono, Preparation of silver-doped rice husk silica composites using the sol-gel method, Ceramics – Silikaty, 66 (**2022**) 3, 365–373, doi:10.13168/cs.2022.0032

[26] E. A. Gonzalez, N. Leiva, N. Vejar, M. Sancy, M. Gulppi, M. I. Azocar, G. Gomez, L. Tamayo, X. Zhou, G. E. Thompson, M. A. Paez, Sol-gel coatings doped with encapsulated silver nanoparticles: inhibition of biocorrosion on 2024-T3 aluminum alloy promoted by Pseudomonas aeruginosa, Journal of Materials Research and Technology, 8 (**2019**) 2, 1809–1818, doi:10.1016/j.jmrt.2018.12.011

[27] A. Ablat, L. Hirsch, M. Abbas, Electron beam versus thermal deposition of aluminum top electrode for organic solar cells, Materials Letters, 312 (**2022**), doi:10.1016/j.matlet.2021.131619

[28] L. Shen, Y. Zhang, W. Yu, R. Li, M. Wang, Q. Gao, J. Li, H. Lin, Fabrication of hydrophilic and antibacterial poly(vinylidene fluoride) based separation membranes by a novel strategy combining radiation grafting of poly(acrylic acid) (PAA) and electroless nickel plating, J. Colloid Interface Sci., 543 (**2019**), 64–75, doi:10.1016/j.jcis.2019.02.013

[29] L. Rao, J. Tang, S. Hu, L. Shen, Y. Xu, R. Li, H. Lin, Inkjet printing assisted electroless Ni plating to fabricate nickel coated polypropylene membrane with improved performance, J. Colloid Interface Sci., 565 (**2020**), 546–554, doi:10.1016/j.jcis.2020.01.069

[30] S. D. Kim, W. G. Choe, J. Choi, J. R. Jeong, Preparation and characterization of silver coated magnetic microspheres prepared by a modified electroless plating process, Powder Technology, 342 (**2019**), 301–307, doi:10.1016/j.powtec.2018.09.094

[31] Y. Zhou, Z. Sun, L. Jiang, S. Chen, J. Ma, F. Zhou, Flexible and conductive meta-aramid fiber paper with high thermal and chemical stability for electromagnetic interference shielding, Applied Surface Science, 533 (**2020**), doi:10.1016/j.apsusc.2020.147431

[32] Z. G. Wu, Y. R. Jia, J. Wang, Y. Guo, J. F. Gao, Core-shell SiO2/Ag composite spheres: synthesis, characterization and photocatalytic properties, Materials Science-Poland, 34 (**2016**) 4, 806–810, doi:10.1515/msp-2016-0121

[33] Q. Li, G. Lin, S. Zhang, H. Wang, J. Borah, Y. Jing, F. Liu, Conducting and stretchable emulsion styrene butadiene rubber composites using SiO_2@Ag core-shell particles and polydopamine coated carbon nanotubes, Polymer Testing, 115 (**2022**), doi:10.1016/j.polymertesting.2022.107722

[34] S. Sembiring, A. Riyanto, I. Firdaus, Junaidi, R. Situmeang, Structure and properties of silver-silica composite prepared from rice husk silica and silver nitrate, Ceramics – Silikaty, 66 (**2022**) 2, 167–177, doi:10.13168/cs.2022.0011

[35] K. Pajor, A. Michalicha, A. Belcarz, L. Pajchel, A. Zgadzaj, F. Wojas, J. Kolmas, Antibacterial and Cytotoxicity Evaluation of New Hydroxyapatite-Based Granules Containing Silver or Gallium Ions with Potential Use as Bone Substitutes, International Journal of Molecular Sciences, 23 (**2022**) 13, 7102–7102, doi:10.3390/ijms23137102

[36] Y. Xiao, L. Lang, W. Xu, D. Zhang, Diffusion bonding of copper alloy and nickel-based superalloy via hot isostatic pressing, Journal of Materials Research and Technology, 19 (**2022**), 1789–1797, doi:10.1016/j.jmrt.2022.05.152

[37] X. Liu, G. Wang, J. Wang, X. Gong, J. Chang, X. Jin, X. Zhang, J. Wang, J. Hao, B. Liu, Electrochromic and Capacitive Properties of WO3 Nanowires Prepared by One-Step Water Bath Method, Coatings, 12 (**2022**) 5, 595–595, doi:10.3390/coatings12050595

[38] C.-H. Kuok, W. Dianbudiyanto, S.-H. Liu, A simple method to valorize silica sludges into sustainable coatings for indoor humidity buffering, Sustainable Environment Research, 32 (**2022**) 1, doi:10.1186/s42834-022-00120-3

[39] M. Jose, P. Sienkiewicz, K. Szymanska, D. Darowna, D. Moszynski, Z. Lendzion-Bielun, K. Szymanski, S. Mozia, Influence of Preparation Procedure on Physicochemical and Antibacterial Properties of Titanate Nanotubes Modified with Silver, Nanomaterials, 9 (**2019**) 5, 795–795, doi:10.3390/nano9050795

[40] A. Ishikawa, T. Kato, N. Takeyasu, K. Fujimori, K. Tsuruta, Selective electroless plating of 3D-printed plastic structures for three-dimensional microwave metamaterials, Applied Physics Letters, 111 (**2017**) 18, 183102–183102, doi:10.1063/1.4986203

[41] K. Zhang, C. Wang, Z. Rong, R. Xiao, Z. Zhou, S. Wang, Silver coated magnetic microflowers as efficient and recyclable catalysts for catalytic reduction, New Journal of Chemistry, 41 (**2017**) 23, 14199–14208, doi:10.1039/c7nj02802d

[42] C. Li, H. Zhang, Y. Song, L. Cai, J. Wu, J. Wu, S. Wang, C. Xiong, Robust superhydrophobic and porous melamine-formaldehyde based composites for high-performance electromagnetic interference shielding, Colloids and Surfaces A: Physicochemical and Engineering Aspects, 624 (**2021**), doi:10.1016/j.colsurfa.2021.126742

[43] T.-T. Li, Y. Wang, H.-K. Peng, X. Zhang, B.-C. Shiu, J.-H. Lin, C.-W. Lou, Lightweight, flexible and superhydrophobic composite nanofiber films inspired by nacre for highly electromagnetic interference shielding, Composites Part A: Applied Science and Manufacturing, 128 (**2020**) C, 105685–105685, doi:10.1016/j.compositesa.2019.105685

[44] F. Ren, Z. Z. Guo, H. Guo, L. C. Jia, Y. C. Zhao, P. G. Ren, D. X. Yan, Layer-Structured Design and Fabrication of Cyanate Ester Nanocomposites for Excellent Electromagnetic Shielding with Absorption-Dominated Characteristic, Polymers, 10 (**2018**) 9, 933–933, doi:10.3390/polym10090933

[45] F. Ren, H. Guo, Z. Z. Guo, Y. L. Jin, H. J. Duan, P. G. Ren, D. X. Yan, Highly Bendable and Durable Waterproof Paper for Ultra-High Electromagnetic Interference Shielding, Polymers, 11 (**2019**) 9, 1486–1486, doi:10.3390/polym11091486

[46] L.-P. Wu, Y.-Z. Li, B.-J. Wang, Z.-P. Mao, H. Xu, Y. Zhong, L.-P. Zhang, X.-F. Sui, Electroless Ag-plated sponges by tunable deposition onto cellulose-derived templates for ultra-high electromagnetic interference shielding, Materials & Design, 159 (**2018**), 47–56, doi:10.1016/j.matdes.2018.08.037

[47] S. Naseer, M. Aamir, M. A. Mirza, U. Jabeen, R. Tahir, M. N. K. Malghani, Q. Wali, Synthesis of Ni-Ag-ZnO solid solution nanoparticles for photoreduction and antimicrobial applications, RSC Adv., 12 (**2022**) 13, 7661–7670, doi:10.1039/d2ra00717g

[48] T. Liu, D. Li, D. Yang, M. Jiang, An improved seed-mediated growth method to coat complete silver shells onto silica spheres for surface-enhanced Raman scattering, Colloids and Surfaces A: Physicochemical and Engineering Aspects, 387 (**2011**) 1, 17–22, doi:10.1016/j.colsurfa.2011.07.030

[49] M. Zhu, G. Xie, L. Liu, P. Yang, H. Qu, C. Zhang, Influence of Mechanical Grinding on Particle Characteristics of Coal Gasification Slag, Materials, 15 (**2022**) 17, 6033–6033, doi:10.3390/ma15176033

[50] Y. Liu, Y. Zhou, Y. Lin, G. Jia, One-pot microwave-assisted synthesis of Ag2Se and photothermal conversion, Results in Physics, 38 (**2022**), doi:10.1016/j.rinp.2022.105590

[51] Y. Da, J. Liu, Z. Gao, X. Xue, Studying the Influence of Mica Particle Size on the Properties of Epoxy Acrylate/Mica Composite Coatings through Reducing Mica Particle Size by the Ball-Milled Method, Coatings, 12 (**2022**) 1, 98–98, doi:10.3390/coatings 12010098

[52] E. R. Wainwright, S. V. Lakshman, A. F. T. Leong, A. H. Kinsey, J. A. Gibbins, S. Q. Arlington, T. Sun, K. Fezzaa, T. C. Hufnagel, T. P. Weihs, Viewing internal bubbling and microexplosions in combusting metal particles via x-ray phase contrast imaging, Combustion and Flame, 199 (**2019**), 194–203, doi:10.1016/j.combustflame.2018.10.019

[53] F. Shahzad, M. Alhabeb, C. B. Hatter, B. Anasori, S. M. Hong, C. M. Koo, Y. Gogotsi, Electromagnetic interference shielding with 2D transition metal carbides (MXenes), Science, 353 (**2016**) 6304, 1137–1140, doi:10.1126/science.aag2421

[54] J. T. Orasugh, S. S. Ray, Graphene-Based Electrospun Fibrous Materials with Enhanced EMI Shielding: Recent Developments and Future Perspectives, ACS Omega, 7 (**2022**) 38, 33699–33718, doi:10.1021/acsomega.2c03579

[55] C. Ji, Y. Liu, J. Xu, Y. Y. Li, Y. D. Shang, X. L. Su, Enhanced microwave absorption properties of biomass-derived carbon decorated with transition metal alloy at improved graphitization degree, Journal of Alloys and Compounds, 890 (**2022**), doi:10.1016/j.jallcom. 2021.161834

[56] Y. Liu, J. N. Qin, L. L. Lu, J. Xu, X. L. Su, Enhanced microwave absorption property of silver decorated biomass ordered porous carbon composite materials with frequency selective surface incorporation, International Journal of Minerals, Metallurgy and Materials, 30 (**2023**) 3, 525–535, doi:10.1007/s12613-022-2491-7